

Effect of borehole stress concentration on compressional wave velocity measurements

Xinding Fang^{*1}, Michael Fehler¹, and Arthur Cheng²: ¹Massachusetts Institute of Technology, ²Halliburton

Summary

Formation elastic properties near a borehole may be altered from their original state due to the stress concentration around the borehole. This could lead to a biased estimation of formation elastic properties measured from sonic logging data. To study the effect of stress concentration around a borehole on sonic logging, we first use an iterative approach, which combines a rock physics model and a finite-element method, to calculate the stress-dependent elastic properties of the rock around a borehole when it is subjected to an anisotropic stress loading. Then we use the anisotropic elastic model obtained from the first step and a finite-difference method to simulate the acoustic response in a borehole. Our numerical results are consistent with published laboratory measurements of the azimuthal velocity variations caused by borehole stress concentration. Both numerical and experimental results show that the variation of P-wave velocity versus azimuth has broad maxima and cusped minima, which is different from the presumed cosine behavior. This is caused by the preference of the wavefield to propagate through a higher velocity region.

Introduction

Borehole acoustic logging data provide an important way to interpret formation elasticity (Mao, 1987; Sinha and Kostek, 1995). Monopole and cross-dipole measurements are widely used for determining the formation P-wave velocity and S-wave anisotropy (Sinha and Kostek, 1995; Sinha and Kostek, 1996; Tang et al., 1999; Tang et al., 2002; Winkler et al., 1998). Most unfractured reservoir rocks, such as sands, sandstones and carbonates, show very little intrinsic anisotropy in an unstressed state (Wang, 2002). However, the stress-induced anisotropy, which is caused by the opening or closing of the compliant and crack-like parts of the pore space due to tectonic stresses, significantly affects the elasticity of rocks. Drilling a borehole in a formation strongly alters the local stress distribution. When the *in situ* stresses are anisotropic, drilling causes the closure or opening of cracks in the formation around a borehole and leads to an additional stress-induced anisotropy. Winkler (1996) experimentally measured the azimuthal P-wave velocity (V_p) variation around a borehole that was subjected to a uniaxial stress loading and showed that the borehole stress concentration has a strong impact on the velocity measurements.

Several approaches have been proposed to calculate the stress-related anisotropy around a borehole. The first approach (Sinha and Kostek, 1996; Winkler et al., 1998) uses the acoustoelastic model to calculate the stress-

induced azimuthal velocity changes around a borehole. The velocity variation with applied stresses is accounted for through the use of the third order elastic constants. The second approach (Tang and Cheng, 2004; Tang et al., 1999) uses an empirical stress-velocity coupling relation to estimate the variation of shear elastic constants (C_{44} and C_{55}) as a function of stress. In this approach, the square of the shear wave velocities propagating along a borehole with different polarizations are assumed to be linearly proportional to the stresses applied normal to the borehole axis. However, these two approaches have no rock physics basis as they ignore the constitutive relationship between an anisotropic applied stress field and the stiffness tensor of a rock (Brown and Cheng, 2007). Brown and Cheng (2007) propose the third approach to calculate stress-induced anisotropy around a borehole embedded in an anisotropic medium. In their model, the stress-dependent stiffness tensor of anisotropic rocks is calculated using a general fabric tensor model (Oda, 1986; Oda et al., 1986). The intrinsic relation between stress and stiffness of a rock is accounted for through the use of a rock physics model, which is not included in the methods of Sinha and Kostek (1996) and Tang (1999). The approach of Brown and Cheng (2007) reflects the physics of stress-induced anisotropy. However, the general fabric tensor model requires prior knowledge of the crack geometries and distributions, which may not always be available in the field applications. Fang et al. (2012) modified the approach of Brown and Cheng (2007) and proposed to use the model of Mavko et al. (1995) to replace the general fabric tensor model. Instead of specifying the crack geometry and distribution, they use the data of V_p and V_s versus hydrostatic pressure to calculate the crack compliance of a rock and then use it to estimate the borehole stress-induced anisotropy.

To understand the effect of borehole stress concentration on borehole sonic logging, a thorough analysis of the propagation of waves in a three dimensional borehole model needs to be conducted. The elasticity of the formation around a borehole is described by the stiffness tensor that is governed by the constitutive relation between the stress field applied around a borehole and the elasticity of a rock with micro-cracks embedded in the matrix. However, there is a lack of wave propagation simulation in all previous studies on this subject. To fill in this gap, we first use the method of Fang et al. (2012) to calculate the stiffness tensor of the formation around a borehole when it is subjected to a stress loading. Then we use a finite-difference method to simulate the wave propagation in the borehole.

Stress effect on sonic logging

Model building

We will compare our numerical simulations with the experiments of Winkler (1996), in which V_P versus azimuth around a borehole in a Berea sandstone sample with and without applied uniaxial stress is measured. In his experiment, a block of Berea sandstone sample having dimensions of $15 \times 15 \times 13$ cm and with a 2.86 cm diameter borehole parallel to the short dimension is placed in a water tank for conducting acoustic measurements. V_P at each azimuth is measured along the borehole axis by using a directional transducer and two receivers. V_P is calculated from the travel time delay of the refracted P-waves recorded at the two receivers, which are 7 and 10 cm, respectively, away from the transducer. The porosity of his Berea sandstone sample is 22%. V_P variation with azimuth is very small before applying the stress, and its average value is about 2540 m/s at no stress state. In his experiment, the center frequency of the received acoustic signals is about 250 kHz.

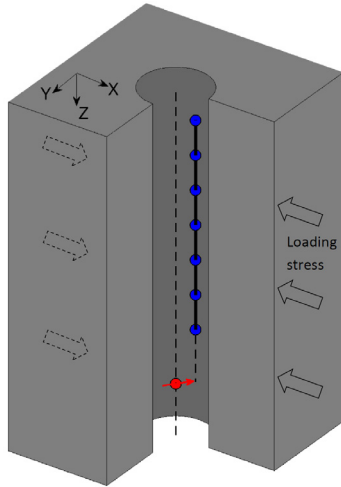


Figure1: Model geometry. Red and blue circles are source and receivers, respectively. Uniaxial stress is applied in the X direction.

V_P and V_S of the rock sample versus hydrostatic pressure, which are the necessary input for the approach of Fang et al. (2012), were not measured by Winkler (1996). We use the data measured from another Berea sandstone sample, which has similar properties to the sample used in the experiment of Winkler (1996), to construct a model for wave propagation simulation. V_P and V_S of our rock sample are 2830 m/s and 1750 m/s, respectively, in an unstressed state. ρ is 2198 kg/m^3 . Porosity is 17.7%. We build a 20 cm borehole model by up scaling the experiment configuration of Winkler (1996) based on the ratio of wave length to borehole diameter, so that the numerical results are comparable to the laboratory measurements. There are two steps to calculate the elastic properties of the rock around a borehole. First, we take a core sample from our Berea

sandstone sample and measure V_P and V_S at different hydrostatic pressures. These data are shown in Fang et al. (2012). Second, we use the data measured in the first step and the method of Fang et al. (2012) to calculate the stiffness tensor of the rock around a borehole when it is subjected to a given stress loading, which is a uniaxial stress applied normal to the borehole axis in the experiment of Winkler (1996).

Figure 1 shows the geometry of our borehole model. The formation is Berea sandstone and the borehole is water saturated. A 20 cm Borehole is at the center of the model along the Z direction. A uniaxial stress is applied normal to the borehole in the X direction. The direction of applied uniaxial stress is defined as 0° . A 4 cm diameter piston source (red circle), which mimics the 1/4 inch diameter directional transducer in the experiment of Winkler (1996), is used in the simulation. Source time function is a Ricker wavelet with a 30 kHz center frequency, which is comparable to the source frequency in the experiment of Winkler (1996) when it is scaled by the borehole diameter. For a given source direction, receivers, which are shown as the blue circles in Figure 1, are 5 cm away from the borehole axis along the source direction.

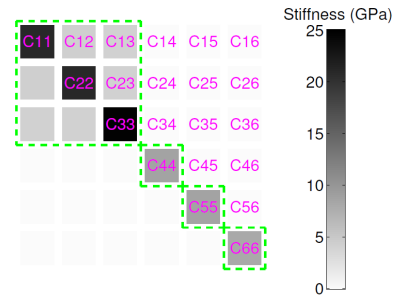


Figure 2: Color hue of each box indicates the average value of the corresponding component (C_{ij}) in the stiffness tensor of the formation around a borehole under 10 MPa stress loading.

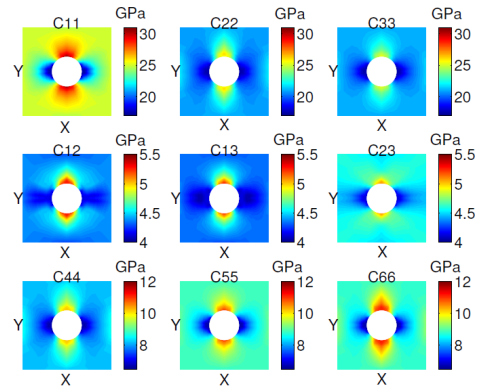


Figure 3: Variations of the nine dominant stiffness components on the X-Y plane for 10 MPa uniaxial stress applied in the X direction.

Stress effect on sonic logging

The elastic model obtained from the method of Fang et al. (2012) contains 21 independent elastic constants, which are functions of the applied stress and position. For 10 MPa stress loading, we calculate the average value of the stiffness tensor of the formation around the borehole and plot it in Figure 2. Color intensity of each box in Figure 2 represents the average value of the corresponding component in the stiffness tensor. The nine components inside the dashed green lines of Figure 2 are about two orders of magnitude larger than the others. This indicates that only 9 elastic constants in the stiffness tensor are important and the rest can be neglected in the simulation. In the simulation below, we only use the 9 dominant components and assume the other components in the stiffness tensor are equal to zero. Figure 3 shows the variations of the 9 dominant elastic constants around the borehole on the X-Y plane for 10 MPa uniaxial stress. Properties of the model are invariant in the Z direction because of model symmetry. As seen in Figure 3, the rock around the borehole becomes inhomogeneous and anisotropic under a stress loading. Due to stress concentration at $\pm 90^\circ$, stiffness of the rock increases from the stress loading direction (0°) to the direction normal to the loading stress ($\pm 90^\circ$).

Numerical simulations

In our simulation, we use a staggered grid finite-difference method with fourth-order accuracy in space and second-order accuracy in time (Cheng et al., 1995). The grid spacing is 0.125 cm (1/160 borehole diameter) and time sampling is 0.125 μ s. Numerical grid dispersion (Moczo et al., 2000) at 30 kHz is smaller than 0.01% for both P- and S-waves in all directions.

Figure 4 shows the data recorded at two receivers located at $z=0.49$ and 0.7 m (source at $z=0$ m), which correspond to the near and far receivers in the experiment of Winkler (1996), for sources at ten different orientations. At each source direction, we divide the distance between the two receivers by the delay of the refracted P-wave arrival times, which are indicated by the red circles in Figure 4, to get the P-wave velocity. Figure 5 shows the azimuthal variation of the normalized P-wave velocity obtained from the numerical simulations together with the data measured by Winkler (1996) for 10 MPa uniaxial stress. The numerical data (squares) and the measured data (circles) are normalized separately by the corresponding P-wave velocity of the rock sample at zero stress state. As shown in Figure 5, our numerical results can predict the laboratory measurements of Winkler (1996) very well. This indicates that the constitutive relation between the formation stiffness around a borehole and the applied stress field is accounted for correctly in the method of Fang et al. (2012). Figures 6a and 6b show the numerical results and the laboratory measurements of Winkler (1996), respectively,

for 5, 10 and 15 MPa uniaxial stresses. For 5 and 15 MPa uniaxial stresses, Winkler (1996) does not show the original measured data but only the best fits. Winkler (1996) finds that the P-wave measured velocities have broad maxima and cusped minima and can be better fit by using an exponential function instead of a cosine function. Our numerical results shown in Figure 6a have very similar azimuthal variation as the measured data shown in Figure 6b. The overall variation of our numerical results is a little bit smaller than that of the measured data, because the rock sample used in the experiment of Winkler (1996) is more compliant than our rock sample as the porosity of our sample is lower and the velocity before stress applied is higher. Another difference between the numerical results and the measured data presents at 0° and 180° , where the measured velocities for 10 and 15 MPa uniaxial stresses are smaller than that for 5 MPa uniaxial stress. This may be caused by the opening of micro cracks induced by tensile stresses, whose effect becomes significant at large loading stress while is negligible at small loading stress. Crack opening caused by tensile stress is neglected in the method of Fang et al. (2012), so the normalized velocities in the numerical results increase with the increase of loading stress at 0° and 180° .

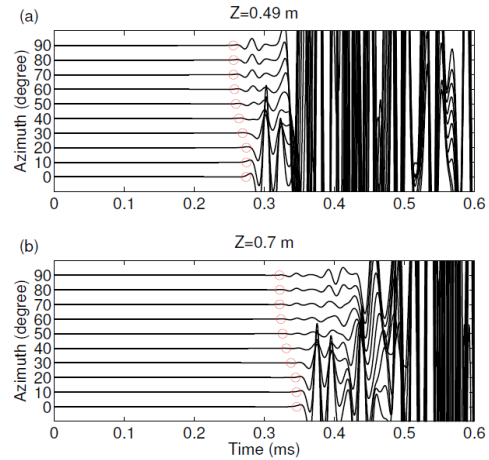


Figure 4: (a) and (b) Seismograms recorded at $z=0.49$ m and 0.7 m, respectively, when the model is subjected to 10 MPa stress loading. Red circles indicate the arrival times of the refracted P-wave. 0° and 90° are along the X and Y axes directions, respectively.

If the propagation of the refracted P-wave follows a straight wave path along the wellbore at the source excitation direction, then the P-wave velocity versus source direction should show a cosine function variation, which has been predicted by the theoretical calculation of Sinha and Kostek (1996) and Fang et al. (2012). The broad maxima and cusped minima shown in both the numerical and measured data in Figure 6 suggest that the propagation of the refracted P-wave does not follow a straight wave path

Stress effect on sonic logging

along the wellbore. A wave tends to propagate through a higher velocity zone and finds the fastest path to reach a receiver. Figure 7 shows the advance of the first break arrival time at each azimuth comparing to that at 0^0 for 5, 10 and 15 MPa uniaxial stresses. At each azimuth, the arrival time advance at a given receiver depth is calculated by subtracting the travel time of the first arrived P-wave at that azimuth from that at 0^0 , where the P-wave arrival time has maximum value as velocity is minimum. The time advance of the first arrived P-wave is zero when z is small, because the first recorded P-waves at near receivers are the direct P-wave, which propagates at water velocity. As shown in Figure 7, the arrival time advance increases with z until it reaches a maximum, which appears at about $z=1.4, 1$ and 0.8 m for 5, 10 and 15 MPa stress loading, respectively. At far receivers near $z=2$ m, the refracted P-waves for sources at all azimuths arrive at almost the same time, because the refracted P-wave propagating through the highest velocity zone at $\pm 90^0$ is faster than that traveling along the wellbore following a straight wave path not at $\pm 90^0$. The maximum of the arrival time advance is associated with the strength of the applied stress which determines the magnitude of the velocity variation around the borehole. This indicates that V_P calculated using the time delay between two receivers depends on the selected positions of the two receivers.

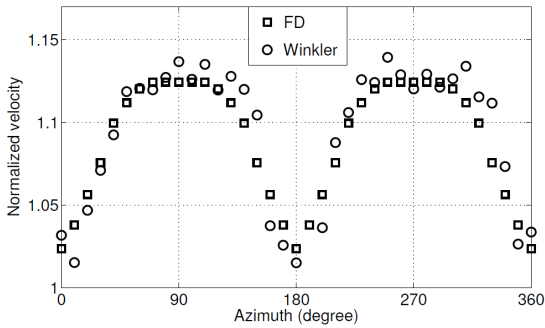


Figure 5: Azimuthal variation of the normalized V_P for 10 MPa uniaxial stress. Squares and circles are V_P obtained from the numerical simulation and the experiment of Winkler (1996), respectively. Applied stress is along 0^0 and 180^0 .

Conclusions

We have studied the azimuthal variation of P-wave velocity caused by borehole stress concentration using a finite-difference method and the method of Fang et al. (2012). We have compared our numerical results with the laboratory measurements of Winkler (1996). The consistency of the azimuthal variation of the normalized V_P between the numerical and the experimental data suggests that the constitutive relation between an applied stress field and stiffness of the rock around a borehole can be accounted for correctly in the approach of Fang et al. (2012). Due to the preference of the wave field to

propagate through a higher velocity region, the variation curve of P-wave velocity versus azimuth shows broad maxima and cusped minima, which is observed in both the numerical simulations and the laboratory experiments. This suggests that a correct interpretation of the P-wave velocity measured from borehole sonic logging needs to consider the effect of borehole stress concentration which results in azimuthally varying stress-induced anisotropy in the formation around a borehole and deviation of the wave path of the refracted P-wave from a straight wave path along borehole axis direction.

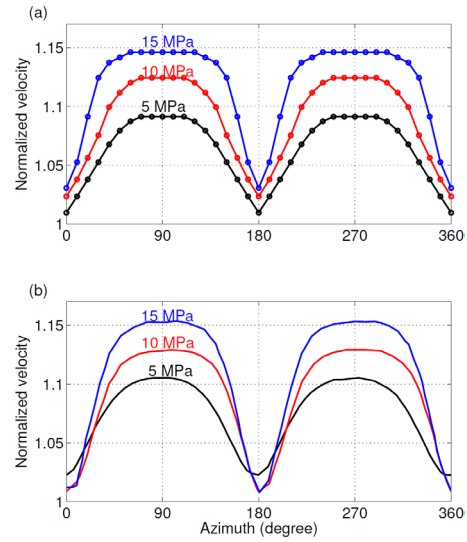


Figure 6: Azimuthal variation of the normalized V_P for three different loading stresses. (a) shows the results obtained from the finite-difference simulations. (b) shows the best fits to the laboratory measured data (modified from Winkler (1996)).

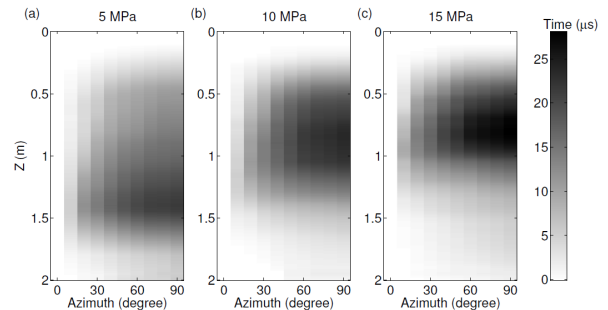


Figure 7: (a), (b) and (c) Advance of the first break arrival time between sources at 0^0 and other directions for 5, 10 and 15 MPa uniaxial stresses, respectively. Horizontal and vertical axes are source direction and receiver depth, respectively.

Acknowledgements

We would like thank Dan Burns, Chen Li and Tianrun Chen for the helpful discussion on sonic logging.

Stress effect on sonic logging

References

- Brown, S., and A. Cheng, 2007, Velocity anisotropy and heterogeneity around a borehole: 77th Annual International Meeting, SEG, Expanded Abstracts, 318-322.
- Cheng, N.Y., C.H. Cheng, and M.N. Toksöz, 1995, Borehole wave propagation in three dimensions: *J. Acoust. Soc. Am.*, **97**, 3483-3493.
- Fang, X.D., M. Fehler, Z.Y. Zhu, T.R. Chen, S. Brown, A. Cheng, and M.N. Toksöz, 2012, Predicting stress-induced anisotropy around a borehole: 82nd Annual International Meeting, SEG, Expanded Abstracts, 1-5.
- Mao, N.H., 1987, Shear wave transducer for stress measurements in boreholes: U.S. Patent 4,641,520.
- Mavko, G., T. Mukerji, and N. Godfrey, 1995, Predicting stress-induced velocity anisotropy in rocks: *Geophysics*, **60**, 1081-1087.
- Moczo, P., J. Kristek, and L. Halada, 2000, 3D fourth-order staggered-grid finite-difference schemes: stability and grid dispersion: *Bulletin of the Seismological Society of America*, **90**, 587-603.
- Oda, M., 1986, An equivalent continuum model for coupled stress and fluid flow analysis in jointed rock masses: *Water Resources Research*, **22**, 1845-1856.
- Oda, M., T. Yamabe, and K. Kamemura, 1986, A crack tensor and its relation to wave velocity anisotropy in jointed rock masses: *Int. Rock Mech. Min. Sci.*, **23**, 387-397.
- Sinha, B.K., and S. Kostek, 1995, Identification of stress induced anisotropy in formations: U.S. Patent 5,398,215.
- Sinha, B.K., and S. Kostek, 1996, Stress-induced azimuthal anisotropy in borehole flexural waves: *Geophysics*, **61**, 1899-1907.
- Tang, X.M., and C. Cheng, 2004, *Quantitative borehole acoustic methods*: Elsevier.
- Tang, X.M., N.Y. Cheng, and A. Cheng, 1999, Identifying and estimating formation stress from borehole monopole and cross-dipole acoustic measurement: SPWLA 40th.
- Tang, X.M., T. Wang, and D. Patterson, 2002, Multipole acoustic logging-while-drilling: SEG Technical Program Expanded Abstracts 2002, 364-367.
- Wang, Z., 2002, Seismic anisotropy in sedimentary rocks, Part 2: laboratory data: *Geophysics*, **67**, 1423-1440.
- Winkler, K.W., 1996, Azimuthal velocity variations caused by borehole stress concentrations: *Journal of Geophysical Research*, **101**, 8615-8621.
- Winkler, K.W., B.K. Sinha, and T.J. Plona, 1998, Effects of borehole stress concentrations on dipole anisotropy measurements: *Geophysics*, **63**, 11-17.